scientific reports

Check for updates

OPEN

Altered neural oscillations and behavior in a genetic mouse model of NMDA receptor hypofunction

David D. Aguilar[1,2]✉, Leana K. Radzik[3], Felipe L. Schiffino[1,2], Oluwarotimi O. Folorunso[2,4], Mark R. Zielinski[1,2], Joseph T. Coyle[2,5], Darrick T. Balu[2,4] & James M. McNally[1,2]

Abnormalities in electroencephalographic (EEG) biomarkers occur in patients with schizophrenia and those clinically at high risk for transition to psychosis and are associated with cognitive impairment. Converging evidence suggests *N*-methyl-D-aspartate receptor (NMDAR) hypofunction plays a central role in the pathophysiology of schizophrenia and likely contributes to biomarker impairments. Thus, characterizing these biomarkers is of significant interest for early diagnosis of schizophrenia and development of novel treatments. We utilized in vivo EEG recordings and behavioral analyses to perform a battery of electrophysiological biomarkers in an established model of chronic NMDAR hypofunction, serine racemase knockout (SRKO) mice, and their wild-type littermates. SRKO mice displayed impairments in investigation-elicited gamma power that corresponded with reduced short-term social recognition and enhanced background (pre-investigation) gamma activity. Additionally, SRKO mice exhibited sensory gating impairments in both evoked-gamma power and event-related potential amplitude. However, other biomarkers including the auditory steady-state response, sleep spindles, and state-specific power spectral density were generally neurotypical. In conclusion, SRKO mice demonstrate how chronic NMDAR hypofunction contributes to deficits in certain translationally-relevant EEG biomarkers altered in schizophrenia. Importantly, our gamma band findings suggest an aberrant signal-to-noise ratio impairing cognition that occurs with NMDAR hypofunction, potentially tied to impaired task-dependent alteration in functional connectivity.

Abnormalities in neural network activity are common across a range of psychiatric disorders and may provide a diagnostic means for early diagnosis[1,2]. A number of electroencephalographic (EEG) biomarkers are associated with impaired cognitive flexibility, attention, executive functioning, and social behavior[3,4]. Of particular interest are disturbances in sensory gating and entrainment to 40 Hz auditory stimuli (auditory steady state response; ASSR), which are impaired in patients with schizophrenia and individuals at high risk to transition to psychosis[5]. Additionally, neural activity abnormalities have been reported in the gamma frequency range (30–80 Hz), either at rest or during cognitive and sensory related task performance[1].

Converging evidence suggests chronic NMDA receptor (NMDAR) hypofunction is central to the pathophysiology of schizophrenia and related psychiatric disorders[6,7]. NMDAR antagonists can transiently recapitulate positive, negative, and cognitive symptoms of schizophrenia in healthy subjects and animal models[8,9], including deficits in EEG biomarkers like the ASSR[10]. These drugs also induce oxidative damage within cortical circuitry[11], potentially disrupting excitatory / inhibitory **(E/I)** balance and causing downstream abnormalities in gamma band oscillations and cognition. Indeed, patients with schizophrenia have well documented impairments in fast-spiking GABAergic interneurons, which may arise from these neurons' increased susceptibility to oxidative damage[12,13]. Antipsychotic treatment can counteract NMDA antagonist-induced changes in some EEG biomarkers, though their therapeutic mechanism is somewhat unclear[14]. Understanding the underlying mechanisms of EEG biomarkers could aid development of new targeted therapies that aim to alleviate cognitive deficits in patients with psychosis[15].

[1]VA Boston Healthcare System, West Roxbury, MA, USA. [2]Department of Psychiatry, Harvard Medical School, Boston, MA, USA. [3]Department of Neuroscience, Stonehill College, Easton, MA, USA. [4]Translational Psychiatry Laboratory, McLean Hospital, Belmont, MA, USA. [5]Laboratory of Psychiatric and Molecular Neuroscience, McLean Hospital, Belmont, MA, USA. ✉email: David_Aguilar@hms.harvard.edu

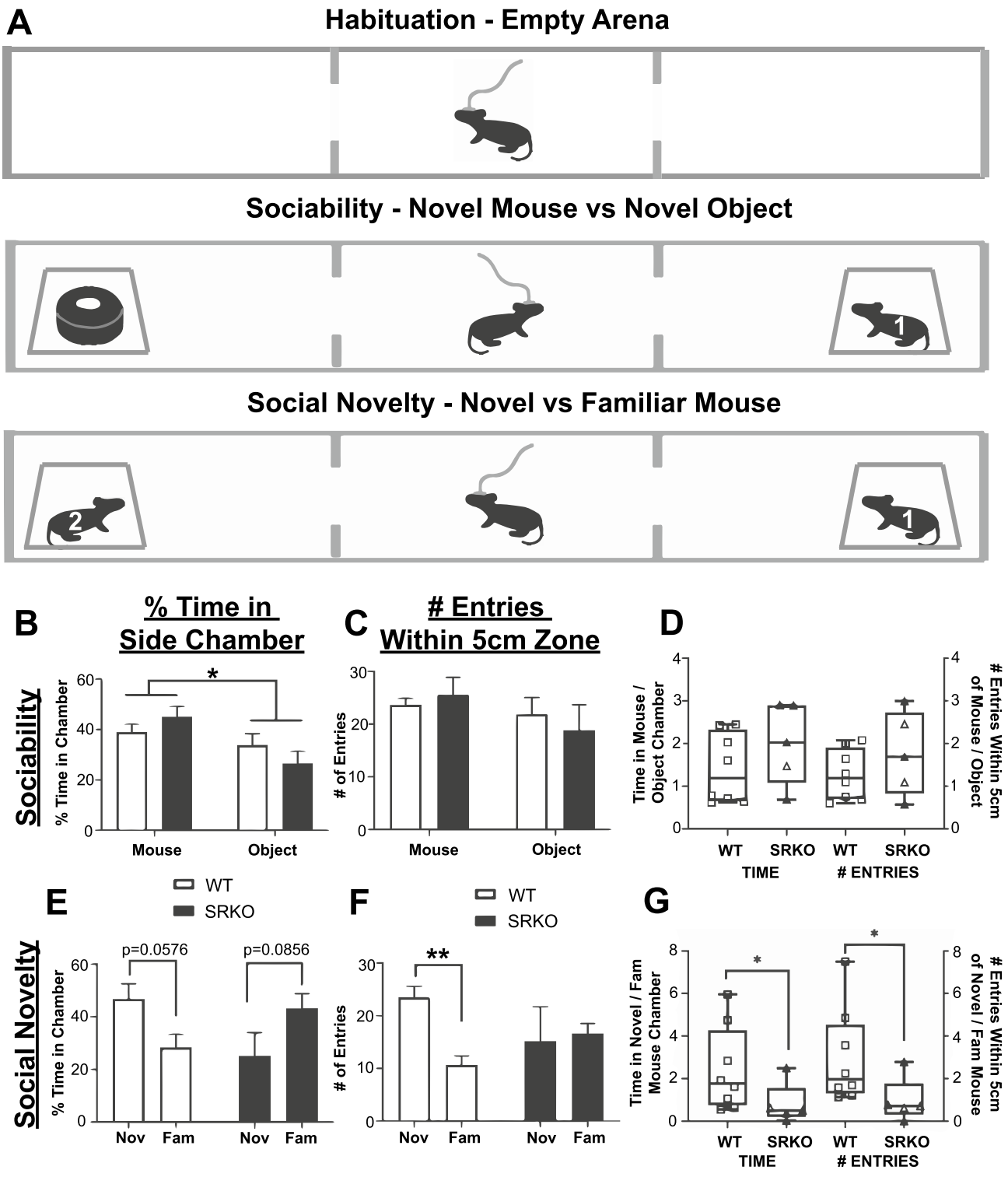
A
Habituation - Empty Arena
Sociability - Novel Mouse vs Novel Object
1
Social Novelty - Novel vs Familiar Mouse
2
1
B
% Time in Side Chamber
Sociability
% Time in Chamber
*
Mouse
Object
C
Entries Within 5cm Zone
of Entries
Mouse
Object
D
Time in Mouse / Object Chamber
Entries Within 5cm of Mouse / Object
WT
SRKO
WT
SRKO
TIME
ENTRIES
E
WT
SRKO
Social Novelty
p=0.0576
p=0.0856
% Time in Chamber
Nov
Fam
Nov
Fam
F
WT
SRKO
**
# of Entries
Nov
Fam
Nov
Fam
G
*
*
Time in Novel / Fam Mouse Chamber
Entries Within 5cm of Novel / Fam Mouse
WT
SRKO
WT
SRKO
TIME
ENTRIES

◂**Figure 1.** Social Novelty Recognition is Impaired in SRKO mice. (**A**) Freely behaving SRKO mice (n = 5) and WT littermates (n = 8) were tethered and placed in a three-chamber arena for a five minute habituation, a ten minute sociability stage (novel mouse "1" vs object), and a ten minute social novelty stage (novel mouse "2" vs familiar mouse "1", see Materials and Methods for detail). During the sociability stage, both WT (white bars) and SRKO mice (black bars) spent a larger percent of time in the chamber containing the novel mouse than the chamber with the novel object (**B**) suggesting the sociability of SRKO mice is unchanged. There were no between-group differences during the sociability stage for either time spent exploring either chamber (**B**), number of entries within a 5 cm zone surrounding the novel mouse or object (**C**), or in the novel mouse/object ratio of these measurements (**D**), indicating WT and SRKO mice behaved similarly during this phase of the task. During the social recognition stage only WT mice spent more time investigating the novel mouse than the familiar mouse, measured by the percent time in each chamber (**E**, strong trend) and the number of entries within a 5 cm zone (**F**). There were significant between-group differences in the novel/familiar mouse ratio for both measurements (**G**), suggesting that WT animals spent a greater proportion of time investigating novel animals than familiar animals when compared to their SRKO littermates. This suggests SRKO mice demonstrate decreased social novelty recognition or impaired social novelty-related exploration. Stars represent a significant main effect (**B**) or a significant Holm–Sidak post hoc test following a significant interaction (**F**) in a two-way ANOVA. Stars in **G** represent a significant Mann–Whitney U test. In all figures, bar graphs represent mean values ± standard error of the mean (see Supplementary Materials B1 for these values) while boxplots represent the median and 25th–75th percentiles with whiskers that represent minimum and maximum values. Individual values are represented in **D** and **G** by hollow squares and triangles. For all experiments the number of stars represents the level of significance (*$p < 0.05$, **$p < 0.01$, ***$p < 0.001$, ****$p < 0.0001$).

Recent genome-wide association studies have identified a number of genetic risk factors for schizophrenia associated with glutamatergic signaling, including the *SRR* gene which encodes serine racemase[16,17]. Here we have examined the relationship between EEG biomarker activity and chronic NMDAR hypofunction by utilizing the serine racemase knockout (SRKO) mouse model. These mice lack expression of the enzyme responsible for synthesis of D-serine, a co-agonist at the NMDAR, and consequently exhibit chronic NMDAR hypofunction[18]. This well-established model exhibits a wide range of schizophrenia-like phenotypes[18–21] and exhibit enhanced oxidative damage and decreased parvalbumin immunoreactivity[22]. We hypothesized that SRKO mice will demonstrate impairments in translationally-relevant EEG biomarkers that are consistent with deficits associated with schizophrenia. The presence of these deficits may help us understand their underlying mechanisms and relationships to long term NMDAR dysfunction.

Material and methods

Animals. SRKO mice were originally generated as described[18]. Adult male and female SRKO (−/−) mice and their wild type (WT) littermates were bred in-house from heterozygote SR (+/−) breeding pairs. These mice were maintained on a C57BL/6 background and were used for all experiments. Animals were given access to food and water ad libitum and maintained on a 12 h light/dark cycle (lights-on 7 am). All procedures were performed in accordance with the National Institutes of Health guidelines, ARRIVE guidelines, and in compliance with the animal protocols approved by the VA Boston Healthcare System Institutional Animal Care and Use Committee.

Stereotaxic surgery. Adult (postnatal day 70+) mice were deeply anesthetized with isoflurane (5% induction, 1–2% maintenance) and body temperature was maintained with a chemical heating pad throughout the surgery. Epidural EEG screw electrodes (0.10″, Cat No. 8403, Pinnacle Technology Inc., Lawrence, Kansas, USA) were implanted in the skull above the frontal cortex (from bregma: A/P + 1.9 mm, M/L − 1.0 mm) and parietal cortex (A/P − 1.0 mm, M/L + 1.0 mm) with a reference and ground screw implanted above the cerebellum (from lambda, A/P − 1.5 mm, M/L ± 1.3 mm). Animals were given at least 7 days to recover from surgery before any experiments began. EEG/EMG signals were acquired via 3 channel amplifier (Pinnacle Technology), sampled at 2 kHz, and low pass filtered at 200 Hz.

Social task-elicited gamma. We utilized a 3 chamber (Maze Engineers, Boston, MA, USA) task protocol modified from DeVito, et al.[20] portrayed in Fig. 1A. SRKO mice and WT littermates were first tethered for EEG recording, and then provided a 15 min habituation period in their home cage. Mice were then placed in a three-chamber arena under low light conditions (14 lx) to measure sociability and social recognition. Before each of the three consecutive stages of this task (see Fig. 1A), mice were provided a five-minute habituation period in the center chamber. During the empty arena habituation, animals had 5 min to explore all three empty chambers. During the 10-min sociability stage, one side chamber contains an unfamiliar, older sex-matched mouse (stranger "1") in a cage while the opposite chamber contains a similar looking novel object (e.g. a black roll of tape) in a cage. The location of the object and animal were counterbalanced between test animals. During the 10-min social novelty stage the novel object was replaced with an unfamiliar sex-matched mouse (stranger "2", age-matched to stranger 1) and the test animal could investigate the novel ("2") and now familiar ("1") mice.

Post hoc behavioral analysis was performed using video tracking software (Ethovision XT, Noldus) to assess the proportion of time spent in each chamber and the number of entries within 5 cm of each cage. Additionally, this tracking software was used in combination with EEG recording (WinEDR, University of Strathclyde, Glasgow, Scotland) to assess neural activity in freely behaving mice specifically during investigations of the arena, an object, or another mouse (previously described in McNally, et al.[23], see Supplementary Material A1). EEG epochs were extracted around the investigation time, and gamma power (25–58 Hz) was examined immediately after

investigation onset and normalized to a 4 s "baseline" (0–4 s pre-stimulus). This frequency range was selected based upon our preliminary data and previous studies which identified investigation-induced increases in this range[23]. Grand averages were taken across all epochs from all animals for each respective genotype after normalization. All animals expressed a left side preference (% time in chamber) during the empty three chamber habituation task, but the number of chamber entries were equal for left and right sides (See Supplementary Materials A1). The influence of baseline side preference on sociability and social novelty should equalize as the side of stimulus presentation was counterbalanced.

Auditory stimulation. Recordings occurred in each animal's home cage within a sound-attenuated recording chamber (background noise ~ 55 dB). Stimuli were generated by a BK Precision 4052 waveform generator (Yorba Linda, California, USA) using Spike2 software (Cambridge Electronic Design, Cambridge, UK) or WinWCP (University of Strathclyde, Glasgow, Scotland) and were delivered through speakers adjacent to the home cage. Data was collected with a Micro 1401 mkII interface module (CED, Cambridge, UK) and Pinnacle's 3 channel amplifier.

Sensory gating. Following a 10-min tethered habituation period, auditory stimuli were presented as pairs of 80 dB 5 kHz tones of 50 ms duration (n = 100 trials) with an inter-trial interval (ITI) of 6 s and a 500 ms interstimulus interval (ISI). The average event-related potential (ERP) for the first (S1) and second (S2) stimulus were analyzed as described in Featherstone, et al.[24]. Briefly, a waveform average of 100 paired-tone presentations was created from raw EEG records. For each ERP, we measured the maximum positive deflection around 20 ms (P20, 15–30 ms after the tone) and the maximum negative deflection around 40 ms (N40, 25–55 ms) following a 100 ms pre-stimulus baseline correction. See Supplementary Material A2–A3 for more detail.

ASSR. As the ASSR task yielded negative results, these methods and results appear in the Supplementary Material (A4 and Table S1).

Data and statistical analyses. Data analysis was performed using custom scripts written for Matlab 2016a (Natick, MA, USA). Power spectral density (PSD) analysis was performed using the multi-taper method (social task-elicited gamma, resting state gamma[25], Chronux Toolbox, chronux.org) or complex Morlet wavelet analysis (sensory gating, ASSR), as described previously[26]. See Supplementary Material A2 for more detail on time–frequency spectral analysis. Statistical significance was set at $p < 0.05$. Statistical analysis was run using GraphPad Prism (San Diego, California, USA) and generally entailed a two-way ANOVA or two-way repeated-measures ANOVA with any significant interactions followed up by a Holm–Sidak multiple comparisons test. For comparisons between two groups, unpaired two-tailed Welch's t tests were used. If the data failed a Kolmogorov–Smirnov test of normality, then a nonparametric analysis was run instead (Mann–Whitney). Repeated measures correlations were calculated in R using the rmcorr package[27]. Bar graphs represent mean values ± standard error of the mean (reported in Supplementary Material B1) while boxplots represent the 25th–75th percentiles and median with whiskers representing minimum and maximum values.

Results

Social novelty recognition is impaired in SRKO mice. Patients with schizophrenia experience social withdrawal and impaired social and nonsocial recognition memory[28], and deficits in social cognition have been linked to altered E/I balance in the cortex[29,30]. A three-chamber arena was used to assess sociability and social recognition by analyzing the proportion of time spent in each chamber and the number of nose-point entries within 5 cm of each cage (Fig. 1A). During the sociability stage, EEG-tethered mice could investigate a novel mouse or a novel object. Behavioral measures of sociability were not significantly different between WT and SRKO mice. Both WT and SRKO mice spent a larger percent of time in the chamber containing the novel mouse than the chamber with the novel object [Fig. 1B, two-way ANOVA, main effect of object, $F(1,22) = 7.543$, $p = 0.0118$], consistent with prior studies[20,31]. We additionally measured the number of nose point entries in a 5 cm zone surrounding each mouse or object as a complementary analysis. There were no significant differences in the number of entries during the sociability task (Fig. 1C, two-way ANOVA). Using proportions (mouse/object) of the measurements described above, we directly compared the sociability preference between WT and SRKO animals. There were no significant differences between WT and SRKO animals in their preference for a novel mouse over a novel object (Fig. 1D, Welch's t-test).

During the social novelty stage, mice could freely investigate the same mouse in the same location from the sociability stage (familiar mouse) or a novel mouse where the object had been in the prior stage. WT mice had a strong trend to spend a larger percent time in the novel mouse chamber than the familiar mouse chamber, while SRKO mice had a weak trend in the opposite direction [Fig. 1E, two-way ANOVA, interaction $F(1,22) = 8.171$, $p = 0.0091$, (WT) $p = 0.0576$, (KO) $p = 0.0856$]. During the social novelty stage, only WT animals had more entries within 5 cm of the novel mouse than the familiar mouse [Fig. 1F, two-way ANOVA, interaction $F(1,22) = 5.094$, $p = 0.0343$, WT $p = 0.0068$]. Together, these results suggest WT but not SRKO animals spent more time investigating the novel mouse than the familiar mouse. The proportion of time spent in the novel/familiar mouse chamber was greater for WT (median = 1.770) than for SRKO animals (median = 0.505, Mann–Whitney $U = 6$, $p = 0.0451$, Fig. 1G, left side). Similarly, the number of nose point entries in a 5 cm radius of the novel/familiar mouse was greater for WT (median = 1.971) than for SRKO animals (median = 0.7083, Mann–Whitney $U = 5$, $p = 0.0295$, Fig. 1G, right side).

In summary, SRKO animals spent a smaller proportion of time investigating the novel versus familiar mouse compared to controls, indicating SRKO mice have decreased short-term social novelty recognition or impaired

social novelty-related exploration. This is supported by another study using a three-chambered approach task in SRKO mice[31]. Despite reports of hyperactivity in SRKO mice[18], the distance traveled and average velocity were not different between WT and SRKO mice during any stage of this task (Figure S1).

Social task-elicited gamma power is impaired in SRKO mice. We additionally recorded social investigation associated gamma power from the frontal cortex during performance of the social novelty task. Here we observed an increase in low gamma activity corresponding with the start of each novel mouse investigation (Fig. 2A,B,D,E). Thus, we focused our analysis on the first second of these investigations using 0.5 s bins. During the sociability task, SRKO mice exhibited a deficit in social task-elicited low gamma power (25–58 Hz) compared to WT littermates from 0.5 to 1 s after the novel mouse investigation began (Fig. 2C, $t(372) = 2.318$, Holm–Sidak adjusted $p = 0.0415$). Deficits in elicited gamma also emerged during the social recognition task. During the first second of novel mouse investigation, WT animals had a significantly larger increase in elicited low gamma power (25–58 Hz) compared to SRKO animals (Fig. 2F, *0–0.5 s,* $t(332) = 2.896$, Holm–Sidak adjusted $p = 0.0040$; *0.5–1 s,* $t(332) = 3.490$, Holm–Sidak adjusted $p = 0.0011$). Elicited gamma was comparable between genotypes during the object and familiar mouse investigations (Figure S2).

To determine if an improper signal-to-noise ratio of gamma power may contribute to this difference, we compared the background gamma power (0–4 s pre-investigation, 25–58 Hz, percent of total power) between genotypes during novel mouse investigations. During the sociability stage, there was no difference in background gamma between genotypes (Fig. 2G). However, during the social novelty stage, SRKO mice had significantly greater background gamma power (median = 22.64) than WT littermates (median = 19.24, Fig. 2H, Mann–Whitney $U = 1436$, $p < 0.0001$). Furthermore, there were significant inverse correlations between investigation-elicited gamma power and background gamma power for all novel mouse investigations across both trials for WT (Fig. 2I; repeated measures correlation, WT $r = -0.251$, $p = 1.56e{-4}$) and SRKO animals (Fig. 2J; $r = -0.187$, $p = 0.0387$). Altogether, our data show that SRKO have impaired social task-elicited gamma activity in response to investigating a novel mouse, perhaps corresponding to impaired task performance. Enhanced background gamma in SRKO mice may be a contributing factor to their deficit in elicited gamma. However, this appears to be task specific, as no changes in gamma power were observed during resting state activity in a separate context (Figures S3, S4).

Sensory gating is impaired in SRKO mice. Sensory gating is an auditory processing phenomenon impaired in patients with schizophrenia and associated with hallucinations or delusions[5,32]. The frontal cortex grand average ERPs generated by paired tones (S1 & S2) were examined (Fig. 3A). Although N40 was larger in S1 than S2 for all animals, only WT animals had significantly larger P20 and P20–N40 amplitudes in S1 than in S2 (two-way RM ANOVA, $p < 0.05$, Fig. 3B, P20 interaction $F(1,17) = 4.646$, N40 main effect $F(1,17) = 18.33$, Fig. 3C, P20–N40 interaction $F(1,17) = 5.213$, see Supplementary Materials B2). Comparison of S2/S1 and S1–S2 "normalized" ratios revealed impaired sensory gating of P20–N40 amplitude in the frontal cortex of SRKO mice compared to WT littermates [unpaired two-tailed Welch's t-test, Fig. 3D, S2/S1, $t(13.39) = 2.887$, $p = 0.0124$; Fig. 3E, S1–S2, $t(15.40) = 2.256$, $p = 0.039$].

Next, we examined whether there was a sensory gating deficit in evoked gamma power (30–80 Hz), as has been reported in patients with schizophrenia and a mouse model of schizophrenia[33]. As shown in Fig. 4A,B, KO mice also demonstrated impaired sensory gating of frontal cortex gamma power compared to WT [unpaired two-tailed Welch's t-test, $t(10.14) = 2.634$, $p = 0.0247$]. Specifically, ERP2 gamma power was 75% reduced from ERP1 in WT mice, while it was only 42% reduced from ERP1 in SRKO mice. We additionally performed PSD comparisons between genotypes for S1 (ERP1) and S2 (ERP2) across the entire frequency range (0.5–100.5 Hz; Fig. 4C,D). Compared to WT, SRKO animals showed an overall decrease in power during ERP1 (Fig. 4C, 1–1.05 s), but not ERP2 (Fig. 4D, 1.50–1.55 s) [*ERP1* main effect of genotype, two-way RM ANOVA, $F(1,17) = 4.576$, $p < 0.0472$].

Other biomarkers are neurotypical in SRKO mice. Other translationally-relevant electrophysiological biomarkers of schizophrenia investigated, including ASSR and sleep spindles, were unaltered in SRKO mice (see Supplementary Materials A6, B3, and Table S1–S3 for more detail). Elicited and induced (non-phase locked "background") power and 40 Hz phase locking were unchanged in the ASSR task between WT (n = 11) and SRKO (n = 10) mice (Table S1). There were no substantial changes between WT (n = 14) and SRKO (n = 12) animals for the percent time in each sleep/wake vigilance state, the average bout length, or average bout frequency (Table S2). Sleep spindle characteristics (spindle density, amplitude, median and mean duration, median frequency) were not different between WT (n = 7) and SRKO (n = 6) animals (Table S3). In the parietal and frontal cortices, significant differences in EEG frequency power spectra (< 10 Hz) were found between SRKO mice and WT littermates during wake and sleep states in light and dark periods, although these effects were variable (see Supplementary Figures S3 and S4). Parietal cortex data was not significantly different between genotypes for most measurements (see Supplementary Materials B4 and Figure S5).

Discussion

SRKO mice have been well characterized to exhibit behavioral, brain morphological, and neurochemical abnormalities reminiscent of schizophrenia[18–20,34–36]. Thus, we tested whether SRKO mice would phenocopy certain EEG biomarker abnormalities observed in patients with schizophrenia or induced by NMDAR antagonists. Here we observed that SRKO mice exhibit deficits in short-term social recognition that corresponded with impaired investigation-elicited gamma power. Additionally, SRKO mice exhibited sensory gating impairments, in terms of both gamma power and ERP amplitude. However, other biomarkers such as ASSR and sleep spindles were

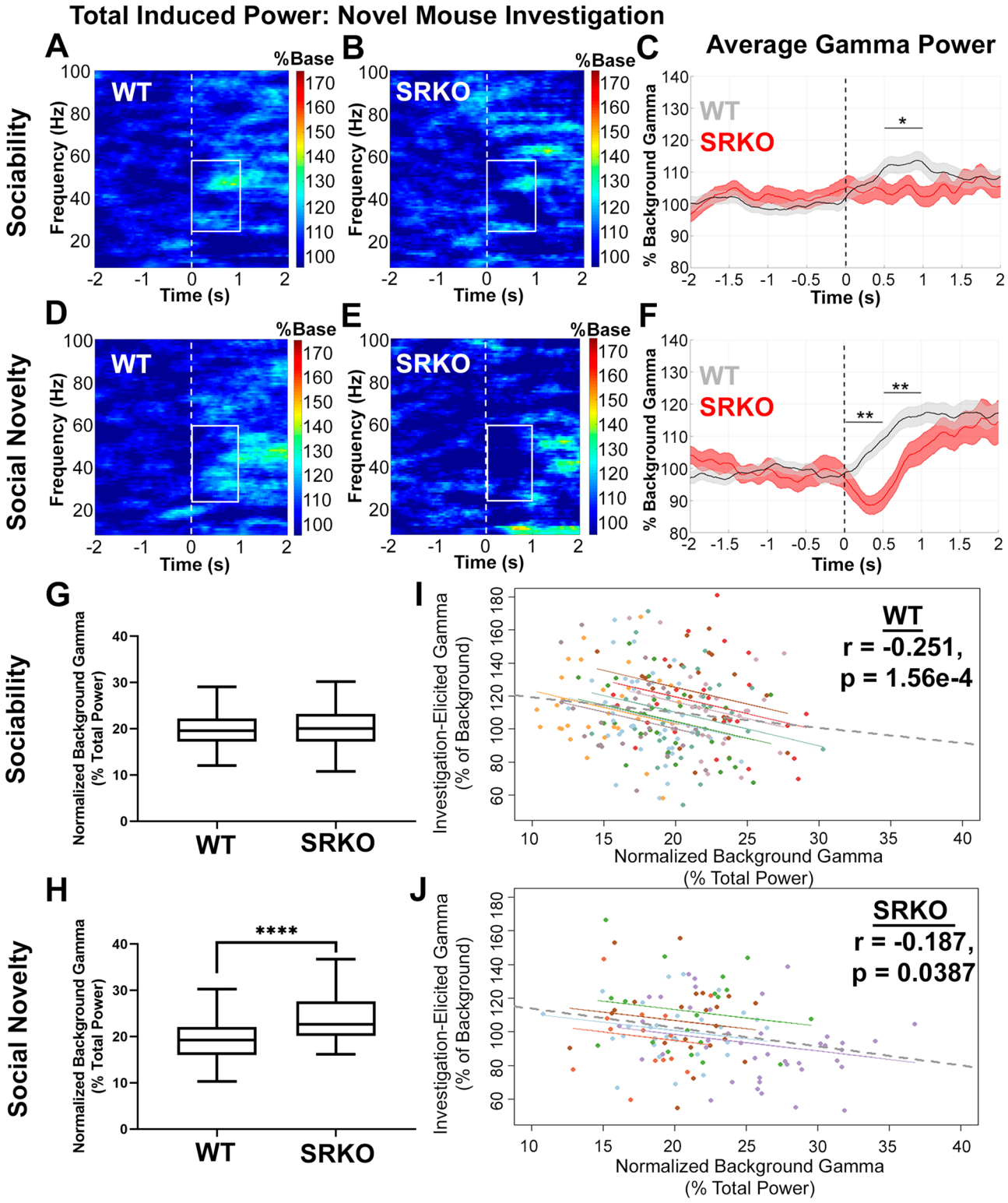
Total Induced Power: Novel Mouse Investigation
A
B
C
Average Gamma Power
Sociability
WT
SRKO
%Base
Frequency (Hz)
Time (s)
% Background Gamma
*
D
E
F
Social Novelty
**
G
H
Normalized Background Gamma (% Total Power)
****
I
J
Investigation-Elicited Gamma (% of Background)
WT
r = -0.251,
p = 1.56e-4
SRKO
r = -0.187,
p = 0.0387

◂**Figure 2.** Social Investigation-Elicited Gamma Power Is Impaired in SRKO mice. Frontal cortex social investigation-elicited gamma power (25–58 Hz) was recorded during the behavioral task described in Fig. 1. Grand average spectrograms appear in (**A**,**B**) and (**D**,**E**) (% of baseline power), while the investigation-elicited gamma power normalized to background gamma is graphed in (**C**) and (**F**). The dotted line represents the start of the novel mouse investigation (time 0) and the white boxes outline the data that was analyzed in 0.5 s bins. WT mice (n = 8) had a significantly larger increase in gamma power than SRKO animals (n = 5) during 0.5–1 s for the sociability task (**C**), and 0–1 s for the social novelty task (**F**). Greater background gamma power (0–4 s prior to novel mouse investigation, percent of total power) was evident in SRKO mice compared to WT littermates during the social novelty task (**H**) but not the sociability task (**G**), suggesting an improper signal-to-noise ratio may contribute to the difference in elicited gamma. Furthermore, there were significant inverse correlations such that greater background gamma power was associated with reduced investigation-elicited gamma power for all novel mouse investigations across both trials for WT (**I**, n = 232 investigations) and SRKO (**J**, n = 127 investigations) animals. In the repeated measures correlations, each dot represents a single investigation of a novel mouse, and each individual mouse is represented by a unique color. The data in Fig. 1 and 2 suggest SRKO mice have a deficit in social-elicited gamma in response to a novel mouse investigation. Enhanced background gamma in SRKO mice may be a contributing factor to this deficit. Stars represent significance from multiple t-tests with Holm–Sidak correction (**C,F**) or a Mann–Whitney U test (**H**).

unaffected in SRKO mice. Abnormal gamma power, whether task-associated or background, was a common theme across our study and may provide insight into the mechanisms behind these biomarker deficits.

Deficient task-associated gamma in SRKO mice is associated with behavioral impairments. Proper E/I balance maintains stable yet flexible cortical activity, and a signal-to-noise ratio necessary for normal cortical function[30]. Deficits in GABAergic interneurons are common in many neuropsychiatric disorders and lead to abnormal gamma band oscillations at rest and during tasks[2]. This likely disturbs E/I balance through cortical disinhibition, leading to "noisier" circuits, and inefficient information processing[30]. Altered gamma oscillations in SRKO mice would suggest chronic NMDAR hypofunction disrupts the E/I balance with consequences on information processing. Indeed, SRKO mice showed impaired task-associated gamma power in the frontal cortex during social recognition and sensory gating tasks which corresponded with deficits in task performance. Patients with schizophrenia often have impaired frontal cortex gamma band oscillations, which are associated with parvalbumin interneuron dysfunction and aberrant cognitive and perceptual functions[2]. Therefore, this deficit might be linked to previously reported reductions in cortical parvalbumin interneuron density in mature adult SRKO mice[22]. In addition, the impaired frontal cortex gamma power that occurred during novel social interactions, but not familiar mouse nor novel object investigations (Figure S2), could be a biomarker for social cognitive dysfunction that indicates a deficit in socially motivated working memory, attention, memory consolidation or retrieval.

We additionally observed that background (pre-investigation) gamma power was abnormally high in the frontal cortex of SRKO mice during performance of the social novelty task (Fig. 2H), but not during independent measurement of gamma at rest (Figure S3A,B). Interestingly, the default mode network (DMN), which is comprised of a collection of brain regions including the prefrontal cortex, exhibits enhanced gamma activity during resting state behavior and suppressed gamma activity during cognitive tasks[37]. Patients with schizophrenia have an impaired ability to suppress the DMN, potentially because of an E/I imbalance, which contributes to working memory deficits and other cognitive impairments[38]. Thus, our findings suggest that SRKO mice may have deficient suppression of background gamma activity during certain behavioral contexts (social investigation) that could result in excess "noise" that disrupts the signal-to-noise ratio and cortical E/I balance, contributing to impaired task performance.

Sensory gating deficits in SRKO mice are similar to schizophrenia. Our sensory gating findings revealed multiple similarities between SRKO mice and patients with schizophrenia. Patients with schizophrenia have a lower S1 P50 amplitude, a comparable or larger S2 P50 amplitude, a larger S2/S1 ratio, and a smaller S1–S2 difference during sensory gating[4,39]. In our study, only WT animals had significant gating of frontal P20 and P20–N40 amplitude (the mouse analogue of the human P50)[40,41]. Therefore, SRKO mice had a larger S2/S1 ratio and a smaller S1–S2 difference similar to what is often seen in patients with schizophrenia. Furthermore, SRKO mice had deficits in frontal cortex evoked power across the gamma frequency range during sensory gating consistent with the clinical schizophrenia literature and another a genetic mouse model relevant to schizophrenia[33]. Normalized beta and gamma power were among frequencies lower in SRKO mice than WT littermates during the period when the ERP1 P20 and N40 occur (0–50 ms). Comparable deficits in beta (20–30 Hz) and gamma power (30–50 Hz) were reported in patients with schizophrenia for the human analogues of these peaks (ERP1 P50 and N100, 0–100 ms), and may be a biomarker of a failed initial sensory registration[39].

Although impaired sensory gating is observed in patients with schizophrenia, pharmacologically-induced NMDAR hypofunction does not usually affect this biomarker. Neither acute nor chronic administration of the NMDAR antagonists ketamine or MK-801 significantly impairs sensory gating (S2/S1 ratio) in humans, mice, or rats[42–44]. Furthermore, mice with reduced NMDAR NR1 subunit expression have a normal sensory gating response despite increased P20 and N40 amplitudes[45], but another group reported a reduced S2/S1 ratio in these mice[46]. Altogether, this suggests the sensory gating deficits observed in SRKO mice may not be due to NMDAR hypofunction alone. Low cortical dopamine levels may contribute to a sensory gating deficit since ketamine (which induces dopamine release[47]) does not induce these deficits[43] and most antipsychotics with D2-antagonist

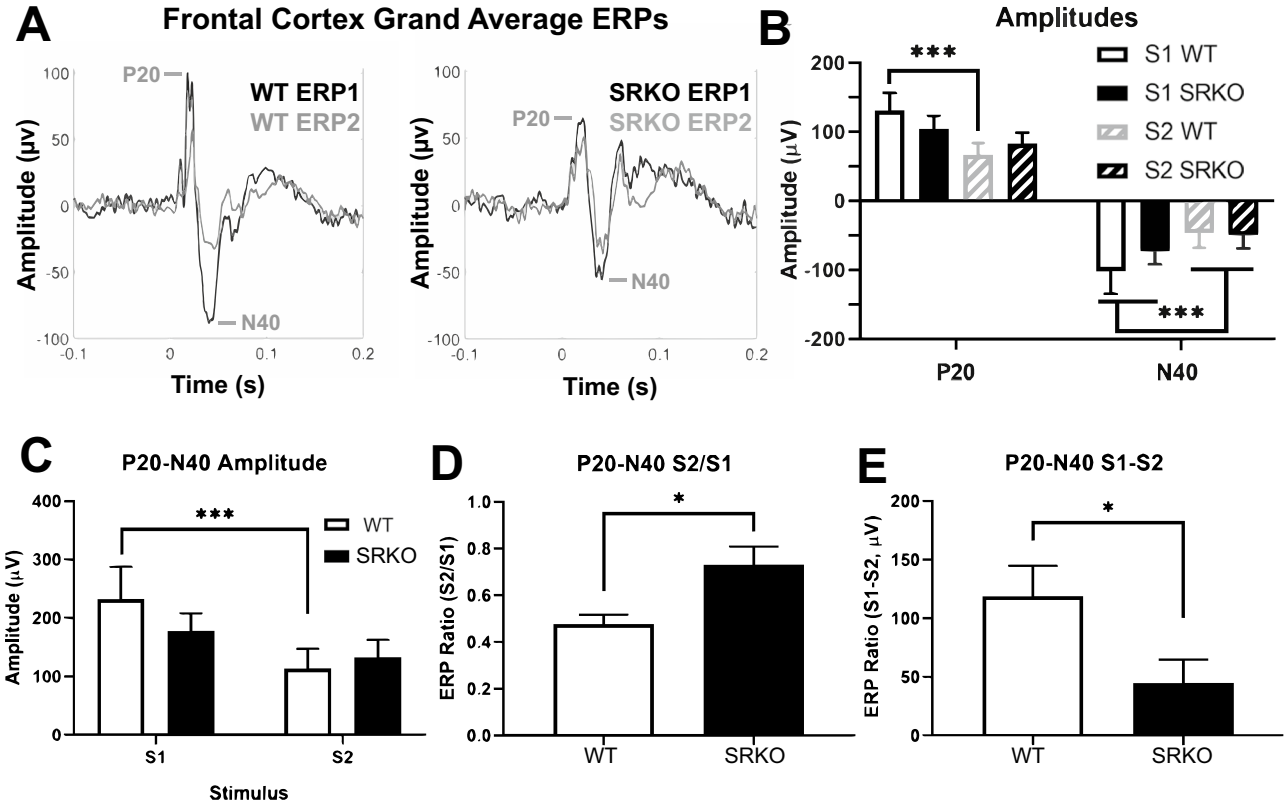

Figure 3. Sensory Gating is Impaired in SRKO mice. Sensory gating was measured in the frontal cortex EEG of SRKO mice (n = 10) and WT littermates (n = 9) by averaging the evoked response potential (ERP) of 100 repetitions of two identical 5 kHz 50 ms tones (S1 and S2) separated by 500 ms. Frontal cortex grand average ERP's are superimposed in (**A**) for WT (**left**) and SRKO (**right**) animals. Although N40 was larger in S1 than S2 for all animals, only WT animals had significantly larger P20 and P20–N40 amplitudes in S1 than in S2 (**B**,**C**). The P20–N40 amplitude was normalized as a ratio between ERP1 (from S1) and ERP2 (from S2) before comparing between groups. Compared to WT littermates, SRKO mice had a reduced gating response of P20–N40 amplitude in the frontal cortex as evidenced by a larger S2/S1 ratio (**D**) and an attenuated difference between S1 and S2 P20–N40 amplitudes (**E**). Stars in (**B**) and (**C**) represent a main effect of stimulus in a two-way RM ANOVA (N40) or significance in a Holm–Sidak post hoc test following a significant interaction in a two-way RM ANOVA (P20, P20–N40). Stars in (**D**) and (**E**) represent significance in an unpaired two-tailed Welch's t-test.

properties fail to rescue these deficits[48]. Mice with reduced alpha-7 nicotinic acetylcholine receptors have sensory gating impairments[33], and clozapine (which enhances acetylcholine[49]) and nicotine each rescue sensory gating deficits in patients with schizophrenia[48,50]. Therefore, reduced cholinergic or cortical dopaminergic activity, as seen in schizophrenia[51,52], may contribute to the sensory gating deficits in schizophrenia and SRKO mice.

ASSR and spindles are unaffected in SRKO mice. Synchronization of cortical neuron firing in response to repetitive stimuli is believed to depend critically on E/I balance and represents a process related to cognitive function[53]. Patients with schizophrenia and rodents administered NMDAR antagonists exhibit abnormalities in their ability to synchronize cortical firing in response to 40 Hz auditory stimuli[26,54]. However, consistent with recently published findings[55], ASSR evoked power was intact in SRKO mice at all measured frequencies (Table S1). Phase locking and background (induced) power were also unchanged at 40 Hz (Table S1). Acute versus chronic NMDAR antagonist treatments have competing effects that may explain our results. In tethered, freely moving rats acute MK-801 altered the intertrial coherence of the 40 Hz ASSR in the primary auditory cortex, but chronic (21 day) MK-801 treatment had no significant effects[56]. Furthermore, the consequences of ketamine on the 40 Hz ASSR in conscious rats depends largely on the dose used, the degree of NMDAR occupancy, and the amount of time since drug administration[57]. Therefore, our neurotypical ASSR result in SRKO mice is compatible with chronic NMDAR antagonist pharmacological studies. This contrasts deficient task-evoked gamma power in other biomarkers; however, these results may arise from distinct mechanisms. Indeed, the 40 Hz ASSR deficit in patients with schizophrenia may be due to enhanced background gamma activity[26], which our mice do not replicate during this task or at rest (Figures S3, S4).

Region specificity could explain why biomarker deficits were seemingly inconsistent and mainly limited to the frontal cortex. The relative expression of SR, D-serine, and glycine in various brain regions could influence NMDAR signaling and the existence or location of biomarker deficits in SRKO mice. If D-serine and glycine

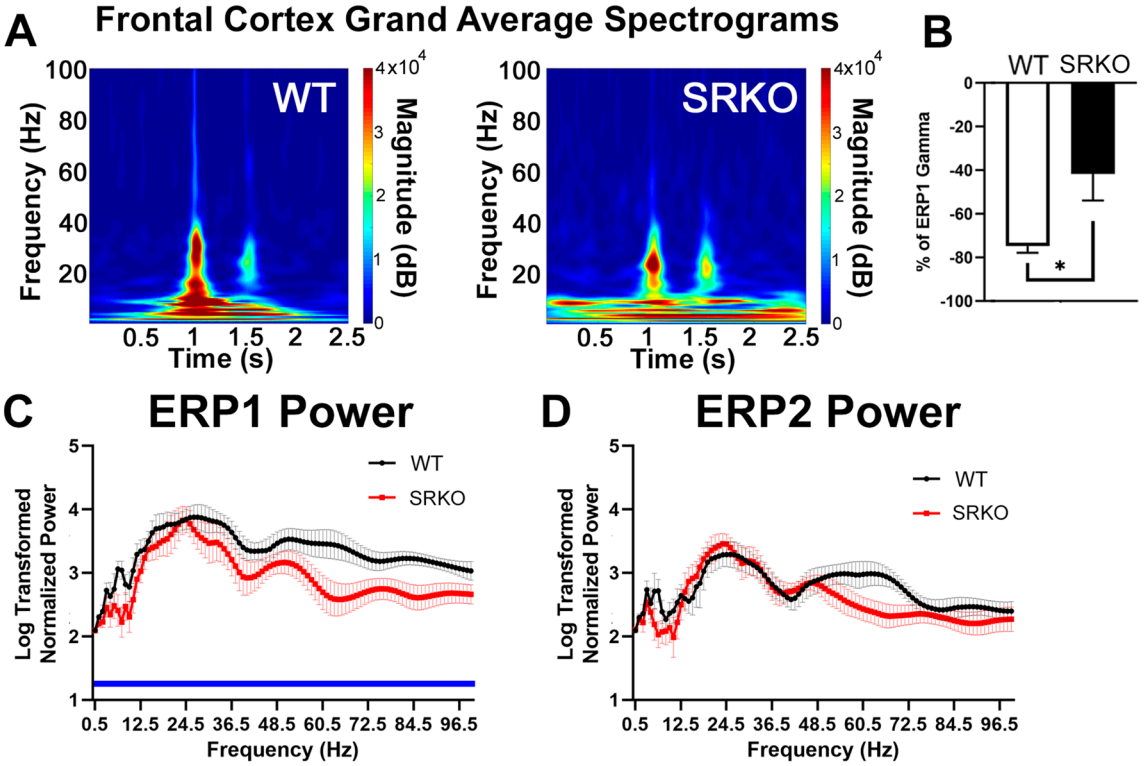

Figure 4. Power Spectral Density Abnormalities Occur in SRKO mice During Sensory Gating. We examined whether there was a sensory gating deficit in evoked gamma power (30–80 Hz). The frontal cortex grand average spectrogram **(A)** demonstrates the change in evoked power during S1 (1–1.05 s) and S2 (1.5–1.55 s) for WT (**left**) and SRKO (**right**) mice. The frequency comparisons in parts (**B**–**D**) were calculated using these stimulus times. Similar to ERP amplitude, SRKO mice also demonstrated impaired sensory gating of gamma power (41.7% reduced from S1 to S2) compared to WT littermates (74.8% reduced, **B**). To examine task-evoked power spectral density differences between genotypes during each stimulus, the log-transformed normalized power for 0.5–100.5 Hz was analyzed using 1 Hz bins. Compared to WT littermates, SRKO animals had decreased power across the frequency spectrum during ERP1 (**C**) but not during ERP2 (**D**). Stars represent a significant unpaired two-tailed Welch's t-test. (**C**) had a main effect of genotype in a two-way RM ANOVA, represented by a blue bar under the significantly different frequencies.

coexist in a brain region, the level of activity can influence which one is used as an NMDAR co-agonist[58]. SRKO mice had no deficits in the 40 Hz ASSR or sleep spindles, which are biomarkers that require intact thalamocortical circuitry[59,60] or normal thalamic NMDAR signaling[61,62]. Regions like the thalamic reticular nucleus do not express high levels of SR ([63]; unpublished data) and thus likely have normal NMDAR function in SRKO mice. Furthermore, NMDAR antagonists have region-specific consequences on gamma power. MK-801 enhances gamma activity in the hippocampus and above bregma but not in the primary auditory cortex of conscious, freely-behaving rats[44]. Conversely, bath application of ketamine onto rat coronal brain slices enhances gamma rhythms (30–50 Hz) in the primary auditory cortex, impairs gamma rhythms in the medial entorhinal cortex, and has no effect on hippocampal slices[64]. Therefore, gamma power in our parietal and frontal electrodes should not necessarily align in our global mouse model of NMDAR hypofunction. Future studies deleting SR in discrete cortical brain regions will address this confound.

NMDAR hypofunction changes delta and theta power. Several observed changes in PSD aligned with NMDAR hypofunction. Chronic NMDAR antagonist treatment can reduce theta and gamma power for weeks or months after the last drug administration in rodents[65,66]. This may explain the SRKO deficit in broadband power during sensory gating and the reduction in parietal cortex normalized power around the theta band (4–7 Hz) during resting state and sleep behaviors for the lights-off (active) period (Figure S4). We also found small differences in EEG delta power (1–4 Hz) during spontaneous NREM sleep, a frequency band that has been reported to be dysregulated with schizophrenia and is involved in cognition[67,68]. NMDAR hypofunction could be involved in certain cognitive impairments observed with schizophrenia through enhanced NREM delta power, as this could potentially interfere with thalamic corollary discharge and information transmission during sleep[69]. However, the largely neurotypical sleep patterns and sleep spindles found in SRKO mice suggest that differences in sleep architecture between genotypes contributed minimally to our cognitive function findings.

Limitations. The social task-elicited gamma experiment had a smaller sample size compared to our other experiments (see Figure Legends and Supplemental Materials). However, social task-elicited gamma power was normalized to background gamma which minimizes inter-mouse variability, and our discovery of lower elicited gamma in SRKO mice during novel mouse investigations was replicated across two trials (sociability and social novelty) suggesting a large effect size. This is supported by clinical and preclinical literature that finds schizophrenia-associated changes in stimulus-evoked gamma are larger and more consistent than changes in resting state gamma[26,70].

Conclusions

In conclusion, the SRKO mouse model mimics a subset of EEG and behavioral phenotypes associated with schizophrenia and chronic NMDAR antagonist treatment. These novel biomarker deficits compliment SRKO literature reporting changes similar to positive, negative, and cognitive symptoms of schizophrenia[18–21,55]. However, other clinically relevant biomarkers that are usually impaired by NMDAR antagonists or disrupted in patients with schizophrenia were not deficient in SRKO mice. These include the auditory steady-state response, sleep spindles, and state-specific power spectral density. Although they do not fully recapitulate symptoms of schizophrenia, these mice may be useful for modeling patients with chronic schizophrenia more accurately than pharmacologic models in specific domains[71] including sensory gating and resting state gamma[70]. Future studies of SRKO mice can confirm whether (1) the abnormal biomarker phenotypes persist among antipsychotic or D-serine treatment, (2) glycine-related compensatory responses are occurring, (3) thalamocortical circuitry is intact, or (4) abnormalities in dopamine levels, cholinergic signaling, or parvalbumin-containing neurons exist in the neocortex. Recent work indicates SRKO mice have reduced inhibitory tone in hippocampal networks which disrupts neural synchrony and the E/I balance[72,73]. This, along with our gamma band findings support the idea of an E/I imbalance manifested as an aberrant signal-to-noise ratio impairing cognition and information processing. This deficit may be tied to impaired task-dependent alteration in functional connectivity and impaired suppression of the DMN. Understanding the mechanisms behind these biomarkers could lead to personalized early interventions that prevent the transition to psychosis.

Supplementary Material accompanies this paper. Supplementary citations include[74,75].

Received: 5 March 2021; Accepted: 9 April 2021
Published online: 27 April 2021

References

1. McNally, J. M. & McCarley, R. W. Gamma band oscillations: A key to understanding schizophrenia symptoms and neural circuit abnormalities. *Curr. Opin. Psychiatry* **29**, 202–210. https://doi.org/10.1097/YCO.0000000000000244 (2016).
2. Gonzalez-Burgos, G., Cho, R. Y. & Lewis, D. A. Alterations in cortical network oscillations and parvalbumin neurons in schizophrenia. *Biol. Psychiatry* **77**, 1031–1040. https://doi.org/10.1016/j.biopsych.2015.03.010 (2015).
3. Cho, K. K. *et al.* Gamma rhythms link prefrontal interneuron dysfunction with cognitive inflexibility in Dlx5/6(+/−) mice. *Neuron* **85**, 1332–1343. https://doi.org/10.1016/j.neuron.2015.02.019 (2015).
4. Toyomaki, A. *et al.* Different P50 sensory gating measures reflect different cognitive dysfunctions in schizophrenia. *Schizophr. Res. Cogn.* **2**, 166–169. https://doi.org/10.1016/j.scog.2015.07.002 (2015).
5. Mikanmaa, E. *et al.* Towards a neurodynamical understanding of the prodrome in schizophrenia. *Neuroimage* https://doi.org/10.1016/j.neuroimage.2017.11.026 (2017).
6. Snyder, M. A. & Gao, W. J. NMDA hypofunction as a convergence point for progression and symptoms of schizophrenia. *Front. Cell Neurosci.* **7**, 31. https://doi.org/10.3389/fncel.2013.00031 (2013).
7. McNally, J. M., McCarley, R. W. & Brown, R. E. Impaired GABAergic neurotransmission in schizophrenia underlies impairments in cortical gamma band oscillations. *Curr. Psychiatry Rep.* **15**, 346. https://doi.org/10.1007/s11920-012-0346-z (2013).
8. Krystal, J. H. *et al.* Subanesthetic effects of the noncompetitive NMDA antagonist, ketamine, in humans. Psychotomimetic, perceptual, cognitive, and neuroendocrine responses. *Arch. Gen. Psychiatry* **51**, 199–214 (1994).
9. Mouri, A., Noda, Y., Enomoto, T. & Nabeshima, T. Phencyclidine animal models of schizophrenia: Approaches from abnormality of glutamatergic neurotransmission and neurodevelopment. *Neurochem. Int.* **51**, 173–184. https://doi.org/10.1016/j.neuint.2007.06.019 (2007).
10. O'Donnell, B. F. *et al.* The auditory steady-state response (ASSR): A translational biomarker for schizophrenia. *Suppl. Clin. Neurophysiol.* **62**, 101–112 (2013).
11. Behrens, M. M. *et al.* Ketamine-induced loss of phenotype of fast-spiking interneurons is mediated by NADPH-oxidase. *Science* **318**, 1645–1647. https://doi.org/10.1126/science.1148045 (2007).
12. Hardingham, G. E. & Do, K. Q. Linking early-life NMDAR hypofunction and oxidative stress in schizophrenia pathogenesis. *Nat. Rev. Neurosci.* **17**, 125–134. https://doi.org/10.1038/nrn.2015.19 (2016).
13. Ruden, J. B., Dugan, L. L. & Konradi, C. Parvalbumin interneuron vulnerability and brain disorders. *Neuropsychopharmacology* https://doi.org/10.1038/s41386-020-0778-9 (2020).
14. Ahnaou, A., Huysmans, H., Van de Casteele, T. & Drinkenburg, W. Cortical high gamma network oscillations and connectivity: A translational index for antipsychotics to normalize aberrant neurophysiological activity. *Transl. Psychiatry* **7**, 1285. https://doi.org/10.1038/s41398-017-0002-9 (2017).
15. Struber, D. & Herrmann, C. S. Modulation of gamma oscillations as a possible therapeutic tool for neuropsychiatric diseases: A review and perspective. *Int. J. Psychophysiol.* **152**, 15–25. https://doi.org/10.1016/j.ijpsycho.2020.03.003 (2020).
16. Schizophrenia Working Group of the Psychiatric Genomics, C. Biological insights from 108 schizophrenia-associated genetic loci. *Nature* **511**, 421–427. https://doi.org/10.1038/nature13595 (2014).
17. Schizophrenia Working Group of the Psychiatric Genomics, C., Ripke, S., Walters, J. & O'Donovan, M. *Mapping genomic loci prioritizes genes and implicates synaptic biology in schizophrenia.* https://doi.org/10.1101/2020.09.12.20192922 *(2020).*
18. Basu, A. C. *et al.* Targeted disruption of serine racemase affects glutamatergic neurotransmission and behavior. *Mol. Psychiatry* **14**, 719–727. https://doi.org/10.1038/mp.2008.130 (2009).
19. Balu, D. T., Basu, A. C., Corradi, J. P., Cacace, A. M. & Coyle, J. T. The NMDA receptor co-agonists, D-serine and glycine, regulate neuronal dendritic architecture in the somatosensory cortex. *Neurobiol. Dis.* **45**, 671–682. https://doi.org/10.1016/j.nbd.2011.10.006 (2012).

20. DeVito, L. M. *et al.* Serine racemase deletion disrupts memory for order and alters cortical dendritic morphology. *Genes Brain Behav.* **10**, 210–222. https://doi.org/10.1111/j.1601-183X.2010.00656.x (2011).
21. Puhl, M. D. *et al.* N-Methyl-d-aspartate receptor co-agonist availability affects behavioral and neurochemical responses to cocaine: Insights into comorbid schizophrenia and substance abuse. *Addict. Biol.* **24**, 40–50. https://doi.org/10.1111/adb.12577 (2019).
22. Steullet, P. *et al.* Oxidative stress-driven parvalbumin interneuron impairment as a common mechanism in models of schizophrenia. *Mol. Psychiatry* **22**, 936–943. https://doi.org/10.1038/mp.2017.47 (2017).
23. McNally, J. M. *et al.* Optogenetic manipulation of an ascending arousal system tunes cortical broadband gamma power and reveals functional deficits relevant to schizophrenia. *Mol. Psychiatry* https://doi.org/10.1038/s41380-020-0840-3 (2020).
24. Featherstone, R. E. *et al.* Mice with subtle reduction of NMDA NR1 receptor subunit expression have a selective decrease in mismatch negativity: Implications for schizophrenia prodromal population. *Neurobiol. Dis.* **73**, 289–295. https://doi.org/10.1016/j.nbd.2014.10.010 (2015).
25. Prerau, M. J., Brown, R. E., Bianchi, M. T., Ellenbogen, J. M. & Purdon, P. L. Sleep neurophysiological dynamics through the lens of multitaper spectral analysis. *Physiology (Bethesda)* **32**, 60–92. https://doi.org/10.1152/physiol.00062.2015 (2017).
26. Hirano, Y. *et al.* Spontaneous gamma activity in schizophrenia. *JAMA Psychiat.* **72**, 813–821. https://doi.org/10.1001/jamapsychiatry.2014.2642 (2015).
27. Bakdash, J. Z. & Marusich, L. R. Repeated measures correlation. *Front. Psychol.* **8**, 456. https://doi.org/10.3389/fpsyg.2017.00456 (2017).
28. Harvey, P. O. & Lepage, M. Neural correlates of recognition memory of social information in people with schizophrenia. *J. Psychiatry Neurosci.* **39**, 97–109. https://doi.org/10.1503/jpn.130007 (2014).
29. Yizhar, O. *et al.* Neocortical excitation/inhibition balance in information processing and social dysfunction. *Nature* **477**, 171–178. https://doi.org/10.1038/nature10360 (2011).
30. Sohal, V. S. & Rubenstein, J. L. R. Excitation-inhibition balance as a framework for investigating mechanisms in neuropsychiatric disorders. *Mol. Psychiatry* **24**, 1248–1257. https://doi.org/10.1038/s41380-019-0426-0 (2019).
31. Matveeva, T. M., Pisansky, M. T., Young, A., Miller, R. F. & Gewirtz, J. C. Sociality deficits in serine racemase knockout mice. *Brain Behav.* **9**, e01383. https://doi.org/10.1002/brb3.1383 (2019).
32. Brockhaus-Dumke, A. *et al.* Sensory gating in schizophrenia: P50 and N100 gating in antipsychotic-free subjects at risk, first-episode, and chronic patients. *Biol. Psychiatry* **64**, 376–384. https://doi.org/10.1016/j.biopsych.2008.02.006 (2008).
33. Smucny, J. *et al.* Evidence for gamma and beta sensory gating deficits as translational endophenotypes for schizophrenia. *Psychiatry Res.* **214**, 169–174. https://doi.org/10.1016/j.pscychresns.2013.07.002 (2013).
34. Balu, D. T. *et al.* Multiple risk pathways for schizophrenia converge in serine racemase knockout mice, a mouse model of NMDA receptor hypofunction. *Proc. Natl. Acad. Sci. U. S. A.* **110**, E2400-2409. https://doi.org/10.1073/pnas.1304308110 (2013).
35. Puhl, M. D. *et al.* In vivo magnetic resonance studies reveal neuroanatomical and neurochemical abnormalities in the serine racemase knockout mouse model of schizophrenia. *Neurobiol. Dis.* **73**, 269–274. https://doi.org/10.1016/j.nbd.2014.10.009 (2015).
36. Balu, D. T. & Coyle, J. T. Chronic D-serine reverses arc expression and partially rescues dendritic abnormalities in a mouse model of NMDA receptor hypofunction. *Neurochem. Int.* **75**, 76–78. https://doi.org/10.1016/j.neuint.2014.05.015 (2014).
37. Grandjean, J. *et al.* Common functional networks in the mouse brain revealed by multi-centre resting-state fMRI analysis. *Neuroimage* **205**, 116278. https://doi.org/10.1016/j.neuroimage.2019.116278 (2020).
38. Anticevic, A. *et al.* The role of default network deactivation in cognition and disease. *Trends Cogn. Sci.* **16**, 584–592. https://doi.org/10.1016/j.tics.2012.10.008 (2012).
39. Nguyen, A. T., Hetrick, W. P., O'Donnell, B. F. & Brenner, C. A. Abnormal beta and gamma frequency neural oscillations mediate auditory sensory gating deficit in schizophrenia. *J. Psychiatr. Res.* **124**, 13–21. https://doi.org/10.1016/j.jpsychires.2020.01.014 (2020).
40. Smucny, J., Stevens, K. E., Olincy, A. & Tregellas, J. R. Translational utility of rodent hippocampal auditory gating in schizophrenia research: A review and evaluation. *Transl. Psychiatry* **5**, e587. https://doi.org/10.1038/tp.2015.77 (2015).
41. Javitt, D. C. & Kantrowitz, J. *Handbook of Neurochemistry and Molecular Neurobiology: Schizophrenia* 3rd edn. (Springer, 2009).
42. Connolly, P. M. *et al.* The effects of ketamine vary among inbred mouse strains and mimic schizophrenia for the P80, but not P20 or N40 auditory ERP components. *Neurochem. Res.* **29**, 1179–1188. https://doi.org/10.1023/b:nere.0000023605.68408.fb (2004).
43. Oranje, B., Gispen-de Wied, C. C., Verbaten, M. N. & Kahn, R. S. Modulating sensory gating in healthy volunteers: The effects of ketamine and haloperidol. *Biol. Psychiatry* **52**, 887–895. https://doi.org/10.1016/s0006-3223(02)01377-x (2002).
44. Sullivan, E. M., Timi, P., Hong, L. E. & O'Donnell, P. Reverse translation of clinical electrophysiological biomarkers in behaving rodents under acute and chronic NMDA receptor antagonism. *Neuropsychopharmacology* **40**, 719–727. https://doi.org/10.1038/npp.2014.228 (2015).
45. Halene, T. B. *et al.* Assessment of NMDA receptor NR1 subunit hypofunction in mice as a model for schizophrenia. *Genes Brain Behav.* **8**, 661–675. https://doi.org/10.1111/j.1601-183X.2009.00504.x (2009).
46. Bickel, S., Lipp, H. P. & Umbricht, D. Early auditory sensory processing deficits in mouse mutants with reduced NMDA receptor function. *Neuropsychopharmacology* **33**, 1680–1689. https://doi.org/10.1038/sj.npp.1301536 (2008).
47. Kokkinou, M., Ashok, A. H. & Howes, O. D. The effects of ketamine on dopaminergic function: Meta-analysis and review of the implications for neuropsychiatric disorders. *Mol. Psychiatry* **23**, 59–69. https://doi.org/10.1038/mp.2017.190 (2018).
48. Adler, L. E. *et al.* Varied effects of atypical neuroleptics on P50 auditory gating in schizophrenia patients. *Am. J. Psychiatry* **161**, 1822–1828. https://doi.org/10.1176/ajp.161.10.1822 (2004).
49. Shirazi-Southall, S., Rodriguez, D. E. & Nomikos, G. G. Effects of typical and atypical antipsychotics and receptor selective compounds on acetylcholine efflux in the hippocampus of the rat. *Neuropsychopharmacology* **26**, 583–594. https://doi.org/10.1016/S0893-133X(01)00400-6 (2002).
50. Chen, X. S., Li, C. B., Smith, R. C., Xiao, Z. P. & Wang, J. J. Differential sensory gating functions between smokers and non-smokers among drug-naive first episode schizophrenic patients. *Psychiatry Res.* **188**, 327–333. https://doi.org/10.1016/j.psychres.2010.12.009 (2011).
51. Weinstein, J. J. *et al.* Pathway-specific dopamine abnormalities in schizophrenia. *Biol. Psychiatry* **81**, 31–42. https://doi.org/10.1016/j.biopsych.2016.03.2104 (2017).
52. Freedman, R., Hall, M., Adler, L. E. & Leonard, S. Evidence in postmortem brain tissue for decreased numbers of hippocampal nicotinic receptors in schizophrenia. *Biol. Psychiatry* **38**, 22–33. https://doi.org/10.1016/0006-3223(94)00252-X (1995).
53. Jardri, R. *et al.* Are hallucinations due to an imbalance between excitatory and inhibitory influences on the brain?. *Schizophr. Bull.* **42**, 1124–1134. https://doi.org/10.1093/schbul/sbw075 (2016).
54. Schuelert, N., Dorner-Ciossek, C., Brendel, M. & Rosenbrock, H. A comprehensive analysis of auditory event-related potentials and network oscillations in an NMDA receptor antagonist mouse model using a novel wireless recording technology. *Physiol. Rep.* **6**, e13782. https://doi.org/10.14814/phy2.13782 (2018).
55. Balla, A., Ginsberg, S. D., Abbas, A. I., Sershen, H. & Javitt, D. C. Translational neurophysiological biomarkers of N-methyl-D-aspartate dysfunction in serine racemase knockout mice. *Biomark. Neuropsychiatry* https://doi.org/10.1016/j.bionps.2020.100019 (2020).
56. Sullivan, E. M., Timi, P., Hong, L. E. & O'Donnell, P. Effects of NMDA and GABA-A receptor antagonism on auditory steady-state synchronization in awake behaving rats. *Int. J. Neuropsychopharmacol* **18**, pyu118. https://doi.org/10.1093/ijnp/pyu118 (2015).

57. Sivarao, D. V. *et al.* 40 Hz auditory steady-state response is a pharmacodynamic biomarker for cortical NMDA receptors. *Neuropsychopharmacology* **41**, 2232–2240. https://doi.org/10.1038/npp.2016.17 (2016).
58. Li, Y. *et al.* Identity of endogenous NMDAR glycine site agonist in amygdala is determined by synaptic activity level. *Nat. Commun.* **4**, 1760. https://doi.org/10.1038/ncomms2779 (2013).
59. Thankachan, S. *et al.* Thalamic reticular nucleus parvalbumin neurons regulate sleep spindles and electrophysiological aspects of schizophrenia in mice. *Sci. Rep.* **9**, 3607. https://doi.org/10.1038/s41598-019-40398-9 (2019).
60. Brenner, C. A. *et al.* Steady state responses: Electrophysiological assessment of sensory function in schizophrenia. *Schizophr. Bull.* **35**, 1065–1077. https://doi.org/10.1093/schbul/sbp091 (2009).
61. Wang, X. *et al.* Aberrant auditory steady-state response of awake mice after single application of the NMDA receptor antagonist MK-801 into the medial geniculate body. *Int. J. Neuropsychopharmacol.* **23**, 459–468. https://doi.org/10.1093/ijnp/pyaa022 (2020).
62. Xiao, G. & Llano, D. A. Hitting the right spot: NMDA receptors in the auditory thalamus may hold the key to understanding schizophrenia. *Int. J. Neuropsychopharmacol.* https://doi.org/10.1093/ijnp/pyaa032 (2020).
63. (C)2004 Allen Institute for Brain Science. Allen Mouse Brain Atlas. https://mouse.brain-map.org/; https://mouse.brain-map.org/experiment/show/74357621).
64. Roopun, A. K. *et al.* Region-specific changes in gamma and beta2 rhythms in NMDA receptor dysfunction models of schizophrenia. *Schizophr. Bull.* **34**, 962–973. https://doi.org/10.1093/schbul/sbn059 (2008).
65. Featherstone, R. E. *et al.* Subchronic ketamine treatment leads to permanent changes in EEG, cognition and the astrocytic glutamate transporter EAAT2 in mice. *Neurobiol. Dis.* **47**, 338–346. https://doi.org/10.1016/j.nbd.2012.05.003 (2012).
66. Kittelberger, K., Hur, E. E., Sazegar, S., Keshavan, V. & Kocsis, B. Comparison of the effects of acute and chronic administration of ketamine on hippocampal oscillations: Relevance for the NMDA receptor hypofunction model of schizophrenia. *Brain Struct. Funct.* **217**, 395–409. https://doi.org/10.1007/s00429-011-0351-8 (2012).
67. Wilckens, K. A., Ferrarelli, F., Walker, M. P. & Buysse, D. J. Slow-wave activity enhancement to improve cognition. *Trends Neurosci.* **41**, 470–482. https://doi.org/10.1016/j.tins.2018.03.003 (2018).
68. Zhang, Y., Quinones, G. M. & Ferrarelli, F. Sleep spindle and slow wave abnormalities in schizophrenia and other psychotic disorders: Recent findings and future directions. *Schizophr. Res.* **221**, 29–36. https://doi.org/10.1016/j.schres.2019.11.002 (2020).
69. Lisman, J. Excitation, inhibition, local oscillations, or large-scale loops: What causes the symptoms of schizophrenia?. *Curr. Opin. Neurobiol.* **22**, 537–544. https://doi.org/10.1016/j.conb.2011.10.018 (2012).
70. Bianciardi, B. & Uhlhaas, P. J. Do NMDA-R antagonists re-create patterns of spontaneous gamma-band activity in schizophrenia? A systematic review and perspective. *Neurosci. Biobehav. Rev.* **124**, 308–323. https://doi.org/10.1016/j.neubiorev.2021.02.005 (2021).
71. Takagi, S., Balu, D. T. & Coyle, J. T. Subchronic pharmacological and chronic genetic NMDA receptor hypofunction differentially regulate the Akt signaling pathway and Arc expression in juvenile and adult mice. *Schizophr. Res.* **162**, 216–221. https://doi.org/10.1016/j.schres.2014.12.034 (2015).
72. Jami, S. A. *et al.* Increased excitation-inhibition balance due to a loss of GABAergic synapses in the serine racemase knockout model of NMDA receptor hypofunction. https://doi.org/10.1101/2020.09.18.304170 (2020).
73. Ploux, E. *et al.* Serine racemase deletion affects the excitatory/inhibitory balance of the hippocampal CA1 network. *Int. J. Mol. Sci.* https://doi.org/10.3390/ijms21249447 (2020).
74. Uygun, D. S. *et al.* Validation of an automated sleep spindle detection method for mouse electroencephalography. *Sleep* https://doi.org/10.1093/sleep/zsy218 (2019).
75. Mitra, P. & Bokil, H. *Observed Brain Dynamics* (Oxford University Press, 2007).

Acknowledgements

This study was supported by the US Department of Veterans Affairs Biomedical Laboratory Research and Development Service Career Development Awards IK2BX002130 (JMM) and IBX002823A (MRZ), VA Merit Award I01BX004500 (JMM), Stonehill College SURE Fellowship (LKR), NIMH T32-MH016259 (DDA, Martha E Shenton), NIMH F32MH119838 (FLS), Whitehall Foundation #2018-05-107 (DTB), BrightFocus Foundation #A2019034S (DTB), 1R03AG063201-01 (DTB), US-Israel Binational Science Foundation Grant #2019021 (DTB), a subcontract of R01NS098740-02 (DTB), Jeane B. Kempner Postdoctoral Fellowship (OOF), and McLean Presidential Fellowship (OOF). JMM and MRZ are Research Health Scientists at VA Boston Healthcare System, West Roxbury, MA. The contents of this work do not represent the views of the U.S. Department of Veterans Affairs or the United States Government. We would like to thank Dr. Robert W. McCarley for his efforts in forming this productive collaboration, and Yunren Bolortuya for assistance with EEG implantation and sleep scoring.

Author contributions

D.D.A., and J.M.M. conceived and designed the experiments; D.D.A., L.K.R., F.L.S. and J.M.M. performed the experiments and analyzed the data; D.D.A and J.M.M. drafted and revised the manuscript for content. Others: conceived the experiments, interpreted results, and revised the manuscript.

Competing interests

All authors except JTC and DTB declare no competing financial interests in relation to the work described. JTC reports holding a patent on D-serine to treat serious mental disorder that is owned by Massachusetts General Hospital but could yield royalties, and a patent on an AI-based EEG method to predict psychotropic drug response. DTB served as a consultant for LifeSci Capital and received research support from Takeda Pharmaceuticals.

Additional information

Supplementary Information The online version contains supplementary material available at https://doi.org/10.1038/s41598-021-88428-9.

Correspondence and requests for materials should be addressed to D.D.A.